Oyster Reef Restoration May Influence Local Sediment Geochemistry Prior to Introduction of Live Oysters

Ilya Sniff
Grinnell College, sniffily@grinnell.edu

Lee Smee
lsmee@disl.org

Havalend E. Steinmuller
Dauphin Island Sea Lab, hsteinmuller@disl.org

Recommended Citation

GULF AND CARIBBEAN

R E S E A R C H

OYSTER REEF RESTORATION MAY INFLUENCE LOCAL SEDIMENT GEOCHEMISTRY PRIOR TO INTRODUCTION OF LIVE OYSTERS[§]

Ilya Sniff [1,2], Delbert L. Smee [1,3], and Havalend E. Steinmuller [1,3*]

[1]*Dauphin Island Sea Lab, 101 Bienville Blvd., Dauphin Island, AL 36258;* [2]*Grinnell College, 1115 8th Ave., Grinnell, IA 50112;*
[3]*Stokes School of Marine Sciences, University of South Alabama, 307 N. University Blvd., Mobile, AL 36688; *Corresponding author,*
email: hsteinmuller@disl.org

INTRODUCTION

Oyster reefs provide a variety of ecosystem services, including the creation of benthic habitat, filtration of suspended solids from the water column, wave attenuation, protection of neighboring shorelines through erosion control, and regulation of water quality (Dame et al. 1984, Meyer et al. 1997, Chambers et al. 2018). Oyster reefs are 'hotspots' of biogeochemical cycling; restored and natural oyster reefs significantly impact fluxes of carbon, nitrogen, and phosphorus (Chambers et al. 2018). These ecosystem services are facilitated by the physical structure of the vertical oyster reef and biological functioning of the oysters themselves. Despite these numerous services, valued at roughly $99,000/ha/yr, oyster populations are declining (Grabowski et al. 2012). Most areas within North America historically populated by oysters (e.g., the northeastern Gulf coast, the western US coast, Chesapeake Bay) have experienced severe oyster population declines in excess of 90% and oysters have been declared functionally extinct in many of these areas. Globally, oysters are estimated to have experienced an 85% loss in population when compared to historical numbers (Beck et al. 2011).

Within the Gulf Coast, declines in intertidal Eastern oyster (*Crassostrea virginica*) populations are due to a multitude of problems, such as predation, overharvesting, disease, hydrological changes, and reduced water quality (Seavey et al. 2011). Many oyster reef restoration efforts are underway in this region, with over 200 restored oyster reefs documented along the Gulf Coast (La Peyre et al. 2014). A novel method of restoration aimed at decreasing oyster mortality from predators through induction of predatory defenses has been implemented in coastal Alabama (Belgrad et al. 2021). Briefly, oyster spat are exposed to predator exudates from blue crabs (*Callinectes sapidus*) to harden their shells before placement in the field. These 'induced' oysters develop increased shell strength, rendering them more resistant to predators such as oyster drills (Belgrad et al. 2021), and have had 50—300% increased survivorship following deployment in the field (Belgrad et al. 2021). Prior to placement of these oyster spat in the field, oyster shells containing no live oysters are placed on the sediments to create suitable substrate in the form of a base layer.

Although oyster reefs act as biogeochemical 'hotspots,' the effects of a base layer on sediment geochemistry in this area have not been studied. The purpose of our study was to determine how a base layer of oyster shells affected sediment geochemistry at a constructed reef and to establish a geochemical baseline for additional measurements after living oysters are added to the reef. This case study will help ascertain the effects of sediment geochemistry caused by living oysters versus the substrate itself. Sediment pH and calcium carbonate percentage were both expected to rise with the introduction of the oyster reef bed. We also expected to see an increase in silt and clay deposition with increasing depth because this stratification of sediment sizes was previously anecdotally reported (Chambers et al. 2018).

MATERIALS AND METHODS

Study Site

The location of this case study was the Lightning Point Restoration Project in Bayou La Batre, AL (Figure 1A). Lightning Point is located on the coastal edge of a sub—estuary of Mobile Bay, located within the Escatawpa River Basin in southwestern Alabama. The site is a tidally—influenced *Juncus roemerianus*—dominated marsh, with mean tidal ranges of 0.42 m (NOAA Tides and Currents, Station #8739803), and mean salinity of 15.8 (Cedar Point Station, arcos.disl.org). Previous oyster restoration projects have occurred nearby (de Barros et al. 2023).

Experimental Design

The reef bed was constructed via deployment of a base of 900 shell bags, each with an approximate volume of 0.027 m³ (Figure 1B). Three rows of shell bags (at the top, middle, and bottom of the reef) were placed in plastic crates so they could be removed to gain access to the sediment underneath. The reef was oriented parallel to the coastal fringe and covered about 42 m². The vertical distance from the top to bottom of the reef was about 30.5 cm, with the top of the reef exposed at mean lower low water (Figure 1B). Sediment cores were collected via push—core to a depth of 5 cm from 6 locations along the reef parallel
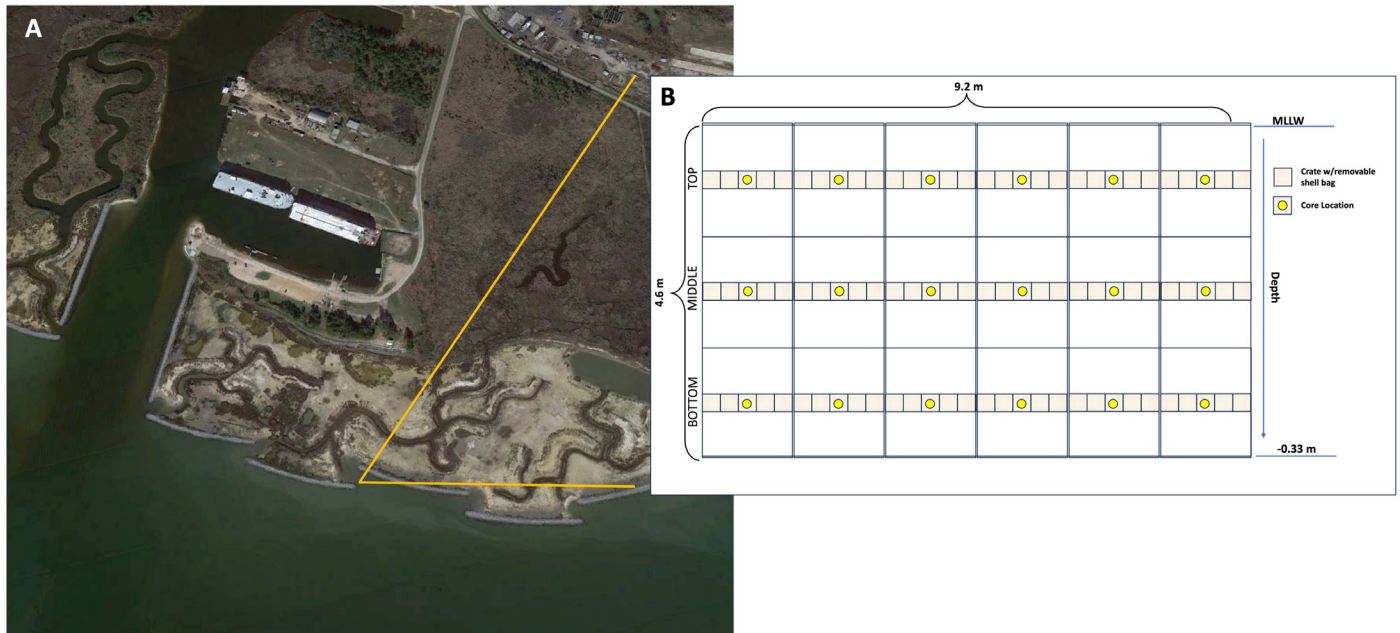
FIGURE 1. *Location and design of oyster reef restoration. A. Google Earth map of approximate location in Bayou La Batre, AL (30.379573 °N, 88.268401 °W). B. Schematic of oyster reef layout. Crates with removable shell bags were placed in the middle of each column and row. Indicated crates at core locations were removed prior to second sampling and then reinstalled post-sampling. MLLW—mean lowest low water.*

to the shoreline at each of 3 different elevations (top, middle, and bottom; Figure 1B) for a total of 18 cores to capture spatial variability in sediment physicochemical characteristics. Sediments were sampled once in May 2023 prior to the reef bed construction, which served as an initial control, and again 47 days after shell bags were deployed. During sampling events, water column salinity and pH were obtained via a YSI ProDSS sonde (Yellow Springs, OH, USA).

Sediment Physicochemical Properties

Sediment pH was determined on field—moist sediment cores. An ~5 g sample of each homogenized core was diluted with dionized water to a 1:5 sediment:water ratio. The samples were stirred and allowed to sit for 30 min before pH and temperature were simultaneously measured with an Accumet XL 200 (Reddy et al. 2013).

Sediment cores were weighed following sampling and homogenized. One subsample (30—60 g) from each core was placed in a drying oven (60°C) for 96 h or until a constant weight was achieved. After drying, subsamples were reweighed to calculate dry bulk density (Reddy et al 2013). The dried subsamples of each core were ground by hand and placed in labeled scintillation vials. Percent organic matter was calculated for each subsample through the loss—on—ignition method; dried sediment samples (2—4 g) in crucibles were placed in a muffle furnace at 550°C for 3 h (Dean 1974). Total mass of each sample was then recorded to calculate percent organic matter. Samples were placed back in the muffle furnace at 990°C for 1 h and total mass was recorded again to determine percent calcium carbonate (Dean 1974). Total carbon and total nitrogen were determined via use of a Costech ECS 4010

CHNSO Analyzer (Valencia, CA, USA).

Dried, ground subsamples were used to determine the relative proportions of sediment grain size. About 10 g of sediment was placed into pre—weighed aluminum sieves with progressively smaller screens (ranging from 2 mm to 63 µm), weighed, and placed on a Humboldt motorized Sieve Shaker (Humboldt Manufacturing Corporation, Elgin, IL, USA) for 10 min (Folk 1980, with modifications). Following shaking, the weight of each sieve and the sample within it was recorded. Initial recorded sieve weight was subtracted from the final sieve weight to determine the mass of each size fraction. Sample mass for each size fraction was then divided by the initial recorded sample mass to determine the relative proportions of each grain size as a percentage. Sediment caught in the 250 µm sieve consisted of material ≥250 µm (medium sand), while sediment caught in the 125 µm sieve consisted of material with sizes between 125–250 µm (fine sand; Wentworth 1922). Similarly, sediment caught in the 63 µm sieve consists of material with sizes between 63–125 µm (very fine sand; Wentworth 1922). The last size class consisted of any material <63 µm (silt + clay; Wentworth 1922).

Statistical Analysis

Heterogeneity of variance and normality for each parameter were verified via Levene's test and the Shapiro—Wilk test, respectively. Datasets that did not meet the assumptions of normality (percent organic matter, total carbon, total nitrogen, percent calcium carbonate, and the medium sand size class) were logarithmically transformed. Means and standard error reported represent back—transformed values. Statistical differences between elevation and sampling times were determined

TABLE 1. *Two-way ANOVA data for all measured characteristics at oyster reef restoration site. Sediment characteristics that demonstrated no significant differences among elevations or sampling times are reported as a homogenized mean. Reported elevation means are temporally homogenized; lowercase letters represent significantly different elevation groups. se—standard error*

	Mean ± 1 se			Elevation		Time	
				p value	F value	p value	F value
Organic Matter (%)	1.760 ± 0.126			0.412	0.914	0.096	2.953
Bulk Density (g/cm)	1.202 ± 0.026			0.654	0.431	0.149	2.199
Total C (g/kg)	0.356 ± 0.030			0.292	1.282	0.228	1.518
Total N (g/kg)	0.026 ± 0.002			0.761	0.276	0.190	1.796
Silt + Clay (%)	18.57 ± 0.710			0.341	1.115	0.910	0.013
	Initial Sampling	**Post-Deployment**		**Elevation**		**Time**	
	Mean ± 1 se	**Mean ± 1 se**		p value	F value	p value	F value
Sediment pH	8.29 ± 0.04	8.86 ± 0.03		0.473	0.767	< 0.0001	110.118
Calcium Carbonate (%)	0.509 ± 0.021	0.818 ± 0.112		0.713	0.342	0.0191	6.137
Medium Sand (%)	1.99 ± 0.16	3.14 ± 0.42		0.451	0.818	0.0164	6.471
	Top	**Middle**	**Bottom**	**Elevation**		**Time**	
	Mean ± 1 se	**Mean ± 1 se**	**Mean ± 1 se**	p value	F value	p value	F value
Fine Sand (%)	52.004[a]	43.68[b]	41.42[b]	0.0053	9.565	0.994	0
Very Fine Sand (%)	27.858[a]	33.88[b]	37.25[b]	<0.0001	25.83	0.462	0.556

using a 2–way ANOVA in R (version 4.1.0; R Foundation for Statistical Computing, Vienna, Austria) with RStudio (version 1.4.1717, PBC, Boston, MA, USA).

Results

Differences among elevations

No significant spatial variation in sediment pH, percent organic matter, percent calcium carbonate, bulk density, total carbon, or total nitrogen was observed either prior to or after the reef bed implementation (Table 1). However, significant differences by elevation were detected in sediment size proportion for the fine sand ($F_{2,33}$ = 9.565, p = 0.0005) and very fine sand size classes ($F_{2,33}$ = 25.83, p < 0.0001). The percent fine sand size class was significantly different between top and middle elevations ($F_{2,33}$ = 9.565, p = 0.002), with a top elevation of 52.00 ± 0.94% and a middle mean of 43.68 ± 2.17%. The top and bottom also saw a significant difference in the fine sand sediment size class ($F_{2,3)}$ = 9.565, p = 0.0023) with a bottom proportion of 41.42 ± 2.04%. There were no significant differences between the middle and bottom elevations for the fine sand size class ($F_{2,33}$ = 9.565, p = 0.6618). The very fine sand size class also saw a significant difference between the top (27.86 ± 0.44%) and middle (33.88 ± 1.15%) elevations ($F_{2,33}$ =

25.83, p = 0.0015) and the top and bottom (37.25 ± 1.05%) elevations ($F_{2,33}$ = 25.83, p < 0.0001), but not the middle and bottom groups ($F_{2,33}$ = 25.83, p = 0.3615).

Differences between sampling times

Sediment pH increased from 8.29 ± 0.04 to 8.86 ± 0.03 between sampling events ($F_{1,34}$ = 110.118, p < 0.0001; Table 1, Figure 2A). Sediment calcium carbonate content was spatially homogenous at each sampling but increased from 0.509 ± 0.021% to 0.818 ± 0.11% between the initial sampling and post–deployment sampling ($F_{1,34}$ = 6.137, p = 0.0191; Table 1,
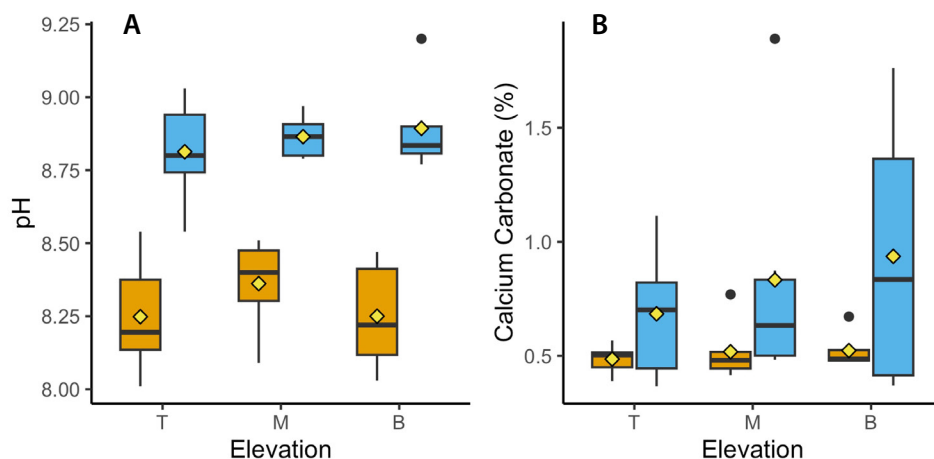
FIGURE 2. *Boxplots denoting sediment characteristics at initial sampling (orange) and post-deployment sampling (blue) by elevation. A. pH. B. Calcium carbonate (%). T—top; M—middle; B—bottom. Boxes and whiskers represent median and interquartile ranges; yellow diamonds denote sample means; black circles denote observations outside 1.5 times the interquartile range.*

Figure 2B). The medium sand sediment size class also saw an increase from 1.99 ± 0.16% to 3.14 ± 0.42% between sampling events ($F_{1,34}$ = 6.471, p = 0.0164; Table 1). Water column pH was 8.19 during the first sampling and 8.30 during the second sampling. Water column salinity was 24.30 and 23.79 at the first and second sampling, respectively.

DISCUSSION

The homogeneity of sediment physicochemical properties prior to the deployment of the reef structure suggests that tidal elevation and the surrounding *Juncus roemerianus*–dominated marsh equally affected all sampling locations in this case study. Thus, observed changes in sediment geochemistry can likely be attributed to the deployment of the reef structure. The exceptions to this assumption were the fine and very fine sand grain size classes, which displayed a greater proportion of the larger size class at the higher elevations, and a greater proportion of the smaller size class (i.e., sand) at the lower elevations. The higher proportion of the fine sand size at the higher elevations situated closer to the marsh platform could be associated with either reduction in flow velocity and turbulence associated with the vegetation interface, which promotes the settling of particles (Christiansen et al. 2000), or resuspension of sediment from higher tidal velocities. The higher proportion of very fine sand at the lower tidal elevations could suggest deposition via settling of these smaller grain sizes facilitated by inputs from marine flow into the system, rather than overland flow draining from the surrounding marsh platform. These differences in grain size observed at different elevations did not persist following the deployment of the reef structure, which suggests that the oyster reef structure in this case exerted more control on sediment grain size distributions than inputs from either the marine environment or the surrounding marsh.

Following the structure deployment, the medium sand sediment size class increased, though this size class remained a minor constituent of overall sediment size distribution. The vertical structure of oyster reefs can increase surface rugosity and enhance trapping of smaller grain size sediments (Styles 2015), although sedimentation rates and materials are also controlled by particle inputs, reef orientation, and hydrodynamics (Lenihan 1999, Colden et al. 2016, Cannon et al. 2022). The limited extent of available data in this case study restricts interpretation of the mechanism controlling the observed changes in the grain size distribution following deployment of the reef

structure herein. Despite this limitation, this study is a first step in contextualizing sedimentation and sediment grain size prior to the deployment of juvenile oysters on this reef and will help inform metrics of oyster reef success because increased sedimentation can negatively affect oyster growth (Adams et al. 1995, Housego and Rosman 2015).

Restoration of oyster reefs has been demonstrated to alter underlying sediment biogeochemistry within 1 year of restoration specifically by increasing sediment total carbon and nitrogen concentrations (Chambers et al. 2018). Within the 47 d period of our study, we saw no significant increase in C or N concentration, indicating many positive geochemical effects of oyster reef restoration are either a) mediated by the presence of live oysters or b) require a longer timescale to develop. However, we did observe increases in sediment pH and calcium carbonate percent, suggesting that the reef structure alters some aspects of sediment physiochemistry within this short timescale and prior to establishment of live oysters. The observed sediment pH increase is attributable to the concurrent increase in calcium carbonate, which was likely deposited by the reef bed through the process of dissolution, ultimately raising the pH through the consumption of H^+. Oysters and oyster spat are particularly vulnerable to low pH systems; low pH significantly decreases oyster survivability (Clark and Gobler 2016). Increasing the pH of local systems could potentially serve to positively affect oyster survivability and increase restoration success.

While the conclusions herein are applicable solely to the novel method of deployment used on the oyster reef in this case study, they demonstrate the importance of reef structure on sediment grain size and physicochemical properties. Our results are subject to the uncertainties inherent within the sampling design, including the potential effects of the plastic crates used to facilitate sampling and the lack of replicability from having a single experimental reef. Our research suggests that many of the previously observed beneficial sediment biogeochemical effects of restoring an oyster reef, such as nutrient sequestration and organics deposition, are likely due to the live oysters themselves rather than the physical introduction of the reef. However, the increased pH and calcium carbonate demonstrated herein represent better conditions for oyster growth and survivability, potentially increasing long term efficacy of oyster reef restoration via this method.

Literature Cited

Adams, M.P., R.L. Walker, and P.B. Heffernan. 1955. The effects of stocking density, bag mesh size, and bottom sediment on the growth and survival of the Eastern oyster, *Crassostrea virginica*, with emphasis on controlling oyster spat fouling. Journal of Applied Aquaculture 4(4):25–44. https://doi.org/10.1300/J028v04n04_03

Beck, M.W., R.D. Brumbaugh, L. Airoldi, A. Carranza, L.D. Coen, C. Crawford, O. Defeo, G.J. Edgar, B. Hancock, M.C. Kay, and H.S. Lenihan. 2011. Oyster reefs at risk and recommendations for conservation, restoration, and management. Bioscience 61:107–116. https://doi.org/10.1525/bio.2011.61.2.5

Belgrad, B.A., E.M. Combs, W.C. Walton, and D.L. Smee. 2021. Use of predator cues to bolster oyster resilience for aquaculture and reef restoration. Aquaculture 538:736553. https://doi.org/10.1016/j.aquaculture.2021.736553

Cannon, D., K. Kibler, L. Walters, and L. Chambers. 2022. Hydrodynamic and biogeochemical evolution of a restored intertidal oyster (*Crassostrea virginica*) reef. Science of The Total Environment 831:154879. https://doi.org/10.1016/j.scitotenv.2022.154879

Chambers, L.G., S.A. Gaspar, C.J. Pilato, H.E. Steinmuller, K.J. McCarthy, P.E. Sacks, and L.J. Walters. 2018. How well do restored intertidal oyster reefs support key biogeochemical properties in a coastal lagoon? Estuaries and Coasts 41:784–799. https://doi.org/10.1007/s12237–017–0311–5

Christiansen, T., P.L. Wiberg, and T.G. Milligan. 2000. Flow and sediment transport on a tidal salt marsh surface. Estuarine, Coastal and Shelf Science 50:315–331. https://doi.org/10.1006/ecss.2000.0548

Clark, H.R. and C.J. Gobler. 2016. Diurnal fluctuations in CO_2 and dissolved oxygen concentrations do not provide a refuge from hypoxia and acidification for early–life–stage bivalves. Marine Ecology Progress Series 558:1–14. https://doi.org/10.3354/meps11852

Colden, A.M., K.A. Fall, G.M. Cartwright, and C.T. Friedrichs. 2016. Sediment suspension and deposition across restored oyster reefs of varying orientation to flow: Implications for restoration. Estuaries and Coasts 39:1435–1448. https://doi.org/10.1007/s12237–016–0096–y

de Barros, M.S., A.R. Rodriguez, A. Bland, and R. Baker. 2023. Assessing habitat enhancement by living shoreline restoration: Exploring potential caveats of nekton community metrics. Restoration Ecology 31(5): e13935. https://doi.org/10.1111/rec.13935

Dame, R.F., R.G. Zingmark, and E. Haskin. 1984. Oyster reefs as processors of estuarine materials. Journal of Experimental Marine Biology and Ecology 83:239–247. https://doi.org/10.1016/S0022–0981(84)80003–9

Dean, W.E. 1974. Determination of carbonate and organic matter in calcareous sediments and sedimentary rocks by loss on ignition: Comparison with other methods. Journal of Sedimentary Research 44:242–248. https://doi.org/10.1306/74D729D2–2B21–11D7–8648000102C1865D

Folk, R.L. 1980. Petrology of Sedimentary Rocks. Hemphill Publishing Company, Austin, TX, USA. 190 p.

Grabowski, J.H., R.D. Brumbaugh, R.F. Conrad, A.G. Keeler, J.J. Opaluch, C.H. Peterson, M.F. Piehler, S.P. Powers, and A.R. Smyth. 2012. Economic valuation of ecosystem services provided by oyster reefs. Bioscience 62:900–909. https://doi.org/10.1525/bio.2012.62.10.10

Housego, R.M. and J.H. Rosman. 2016. A model for understanding the effects of sediment dynamics on oyster reef development. Estuaries and Coasts 39:495–509. https://doi.org/10.1007/s12237–015–9998–3

La Peyre, M., J. Furlong, L.A. Brown, B.P. Piazza, and K. Brown. 2014. Oyster reef restoration in the northern Gulf of Mexico: Extent, methods and outcomes. Ocean and Coastal Management 89:20–28. https://doi.org/10.1016/j.ocecoaman.2013.12.002

Lenihan, H.S. 1999. Physical–biological coupling on oyster reefs: How habitat structure influences individual performance. Ecological Monographs 69:251–275. https://doi.org/10.1890/0012–9615(1999)069[0251:PBCOOR]2.0.CO;2

Meyer, D.L., E.C. Townsend, and G.W. Thayer. 1997. Stabilization and erosion control value of oyster cultch for intertidal marsh. Restoration Ecology 5:93–99. https://doi.org/10.1046/j.1526–100X.1997.09710.x

Reddy, K.R., M.W. Clark, R.D. DeLaune, and M. Kongchum. 2013. Physicochemical characterization of wetland soils. Methods in Biogeochemistry of Wetlands 10:41–54. https://doi.org/10.2136/sssabookser10.c3

Seavey, J.R., W.E. Pine III, P. Frederick, L. Sturmer, and M. Berrigan. 2011. Decadal changes in oyster reefs in the Big Bend of Florida's Gulf Coast. Ecosphere 2(10):1–14.

Styles, R. 2015. Flow and turbulence over an oyster reef. Journal of Coastal Research 31:978–985. https://doi.org/10.2112/JCOASTRES–D–14–00115.1

Wentworth, C.K. 1922. A scale of grade and class terms for clastic sediments. The Journal of Geology, 30:377–392. https://doi.org/10.1086/622910